Available online at www.sciencedirect.com
SCIENCE DIRECT
Journal of Catalysis 227 (2004) 282–296
JOURNAL OF CATALYSIS
www.elsevier.com/locate/jcat

Manganese–lanthanum oxides modified with silver for the catalytic combustion of methane

Andrzej Machocki [a,*], Theophilos Ioannides [b], Beata Stasinska [a], Wojciech Gac [a], George Avgouropoulos [b], Dimitris Delimaris [b], Wieslaw Grzegorczyk [a], Sylwia Pasieczna [a]

[a] *University of Maria Curie-Sklodowska, Faculty of Chemistry, Department of Chemical Technology, 3 Maria Curie-Sklodowska Square, 20-031 Lublin, Poland*
[b] *Foundation for Research and Technology-Hellas, Institute of Chemical Engineering and High Temperature Chemical Processes (FORTH/ICE-HT), P.O. Box 1414, Patras, GR-26500, Greece*

Received 10 March 2004; revised 19 July 2004; accepted 21 July 2004

Available online 24 August 2004

Abstract

The characterization of manganese–lanthanum oxides modified with silver has been performed in order to identify factors responsible for the variation of their activity in the oxidation of methane. A significant increase in the activity per unit surface area in silver-containing catalysts occurred above 800 K, where a new source of surface oxygen appeared. It is probably oxygen released from filled oxygen vacancies, more weakly bound in the oxides structure in comparison with lattice oxide ions, more mobile, and therefore easily accessible to methane oxidation. Such oxygen is probably neighboring with silver ions. The remaining part of the catalyst may constitute a reservoir of oxygen ions with which the vacancies are filled and which is supplemented with the gaseous oxygen. A consequence of filling up oxygen vacancies is the appearance of a larger number of manganese ions in the unstable oxidation state Mn^{4+}. The rate of methane oxidation is a function of the Mn^{4+}/Mn^{3+} surface ratio which is a parameter characterizing the intrinsic properties of the manganese–lanthanum oxides, influencing their activity.

Keywords: Manganese–lanthanum oxides; Silver modifier; Methane; Catalytic combustion

1. Introduction

Interest in the catalytic combustion of methane results mainly from the possibility of lowering the combustion temperature so that minor amounts of nitrogen oxides are produced, smaller than those which remain in the waste gases even after treatment with the most effective methods [1–6]. A catalyst may also make it possible to purify waste gases of methane when they contain such small amounts of methane that they would not undergo ignition in ordinary burners.

Manganese oxides are among the various oxide catalytic materials showing a fairly good activity in flameless methane combustion [1,7–10]. Their heat resistance, and thus also the possibility of industrial utilization, improves when manganese oxide becomes bound in the perovskite structure of the general formula ABO_3, e.g., lanthanum-based perovskite $LaMnO_3$, which is one of the most active perovskite oxide catalysts for the combustion of methane [9–18]. The rare earth metals in the perovskite provide thermal stability of transition metal oxides [9,11,19]. Lanthanum oxide alone also shows activity in the reaction of the complete oxidation of methane, though much lower than manganese oxide [8]. In recent years it has been demonstrated that doping of perovskites $LaNiO_3$, $LaMnO_3$, $LaCoO_3$ [20,21], $LaFeO_3$, and $LaFe_{0.5}O_3$ [22] with silver increases their activity in methane combustion. Moreover, Ag-doped $LaCoO_3$ showed no deactivation in methane combustion during 50 h at 600 °C [20]. Even greater activity

* Corresponding author. Fax: (+48-81) 5375565.
E-mail addresses: machocki@hermes.umcs.lublin.pl (A. Machocki), theo@terpsi.iceht.forth.gr (T. Ioannides).

0021-9517/$ – see front matter
doi:10.1016/j.jcat.2004.07.022

enhancement in comparison with $LaMnO_3$ was observed in the case of composite Ag/Mn/perovskites catalysts in CO oxidation [19,21]. In perovskites some part of basic cations may be replaced by other metal cations with similar ionic radii, with perovskite crystalline structure being almost unaltered. In the case of $LaMnO_3$ silver cations may only replace lanthanum cations (the ionic radii being Ag^+ 1.40 Å, La^{3+} 1.22 Å, Mn^{3+} 0.66 Å, Mn^{4+} 0.56 Å [12]), forming perovskites of the type $La_{1-x}Ag_xMnO_3$. Naturally, such cation exchange must entail the appearance of structural defects compensating the charge and preserving the electroneutrality of the perovskite, which affect its catalytic activity. An increase in the activity of perovskites in the reactions of the full oxidation of CO and hydrocarbons was also obtained following substitution of lanthanum ions by cations of other metals, e.g., Sr, Ca, Ce [9,12,13,15,18,23].

The promoting action of silver is not confined only for perovskites. There have been reports of activity enhancement in CO and VOC oxidation [24–31] after doping of manganese or cobalt oxides—unsupported or supported on Al_2O_3—with silver. It has been suggested that the increased activity of these silver-modified catalysts results from a synergistic interaction between silver oxide and manganese or cobalt oxides and from increase of the lability of lattice oxygen. Manganese–silver and cobalt–silver oxides had a higher activity than each individual catalyst [25,27–29]. Differences in the activities of pure manganese and silver catalysts depended on the accepted basis of comparison. In unsupported catalysts the activity of silver oxide in CO oxidation in reference to its weight was much smaller than that of manganese oxide [25,29] and of cobalt oxide [25,28], but on a surface area basis silver oxide exhibited very high activity [28]. For Al_2O_3-supported catalysts the temperature required for 98% conversion of CO and VOCs on the silver catalyst depended on Ag loading but generally was lower than on the manganese catalyst [27], which is a reverse dependence than in the case of unsupported catalysts.

Silver alone is known to be a good partial oxidation catalyst; it is used in industry for the partial oxidation of methanol to formaldehyde and for the oxidation of ethylene to ethylene epoxide. The reports cited above indicate that silver may also be a catalyst of complete oxidation. Studies [32] also show that silver supported on zirconia may catalyze the complete oxidation of methane (the only oxidation products were carbon dioxide and water). Methane conversion strongly depended on silver state and dispersion: the catalyst activity was higher when metallic Ag crystallites were larger than 10 nm and partially oxidized.

The present paper reports experimental results concerning the preparation, characterization, and activity of silver-modified, manganese–lanthanum oxide composite catalysts in the complete oxidation of methane. The catalysts were prepared by a coprecipitation method with various precipitation agents and by various drying procedures. The characterization of the catalysts was performed by X-ray diffraction, infrared spectroscopy, photoelectron spectroscopy, temperature-programmed reduction, and temperature-programmed oxygen desorption, in order to identify factors responsible for the variation of the catalysts activity and to elucidate the modifying role of silver in these catalysts.

2. Experimental

Catalysts MnLa, 0.1AgMnLa, and 0.3AgMnLa were obtained by coprecipitation from aqueous solutions of nitrates by tetraethylammonium hydroxide ($(C_2H_5)_4NOH$) or ammonium carbonate ($(NH_4)_2CO_3$) as precipitating agents. Digits 0.1 or 0.3 in the catalyst's symbol denote the mole fraction of lanthanum replaced with silver. The precipitated precursors were either dried conventionally at 373 K (catalysts marked with CD—conventional drying) or with supercritical carbon dioxide (catalysts marked with SD—supercritical drying) and calcined at 1073 K for 1 h in air. Prior to supercritical drying, water in the precipitates was exchanged with ethanol. In all experiments the catalysts were applied in the form of powder (mean grain size about 20 μm). The data regarding characterization of catalysts are presented in Table 1.

The bulk contents of manganese, lanthanum, and silver in catalysts were determined by X-ray fluorescence spectroscopy. Pellets for the XRF analysis were prepared by pressing catalysts powder. The measurements were performed by the energy-dispersive XRF spectrometer (Canberra 1510) equipped with the liquid nitrogen-cooled Si(Li) detector. The AXIL software package was used for spectral deconvolution and for the calculation of the component contents of the catalysts.

BET total surface area of the catalysts was measured by argon adsorption at the liquid nitrogen temperature in a static-volumetric glass apparatus, which ensured a vacuum better than 2×10^{-6} kPa.

X-ray powder diffraction patterns of calcined catalysts were collected with an upgraded Zeiss HZG-4 diffractometer using Ni-filtered Cu-K_α radiation. The samples were scanned by a step-by-step technique, at 2θ intervals of 0.05° and a recording time of 10 s for each step. The measured patterns were compared with the JCPDS (Joint Committee on Powder Diffraction Standards) database for phase identification.

The infrared spectra were recorded by means of a Bio-Rad Excalibur FTIR spectrometer at a resolution of 4 cm^{-1} in the fundamental frequencies region where the IR bands are produced by the lattice vibrations of the solid oxides themselves. A sample of a catalyst (5 mg) was mixed and ground in an agate mortar with 400 mg of spectroscopically pure dry potassium bromide to a fine powder and then it was pressed to form a disk less than 1 mm thick. Data were collected in the transmission mode at room temperature under air. Interferograms of 256 scans were averaged for each IR spectrum.

Table 1
Catalyst characterization results

Catalyst	Precipitant[a]	Drying method	Atomic ratio[b]			Phase composition[c]	Surface area (m^2/g)
			Mn	La	Ag		
MnLa-CD	TAOH	Conventional	1	1.07	–	$LaMnO_{3+\delta}$ (main), Mn_2O_3 and/or Mn_3O_4 (v.s.), La_2O_3 and $La(OH)_3$ (v.s.)	17.5
MnLa-SD	TAOH	Supercritical CO_2	1	1.10	–	$LaMnO_{3+\delta}$ (main), Mn_2O_3 and/or Mn_3O_4 (v.s.), La_2O_3 and $La(OH)_3$ (v.s.)	15.7
0.1AgMnLa-CD	$(NH_4)_2CO_3$	Conventional	1	0.91	0.13	$LaMnO_{3+\delta}$ (main), Mn_2O_3 and/or Mn_3O_4 (s.), $La_2O_2CO_3$, La_2O_3, $La(OH)_3$, Ag (tr.)	8.5
0.1AgMnLa-SD	$(NH_4)_2CO_3$	Supercritical CO_2	1	0.96	0.13	$LaMnO_{3+\delta}$ (main), Mn_2O_3 and/or Mn_3O_4 (tr.), La_2O_3, $La(OH)_3$, $La_2O_2CO_3$ (s.), Ag (s.)	11.1
0.3AgMnLa-CD	TAOH	Conventional	1	0.72	0.33	$LaMnO_{3+\delta}$ (main), MnO_2 (v.s.), Mn_2O_3 and/or Mn_3O_4 (tr.), La_2O_3 and $La(OH)_3$ (v.s.), Ag (v.s.)	12.7
0.3AgMnLa-SD	TAOH	Supercritical CO_2	1	0.73	0.34	$LaMnO_{3+\delta}$ (main), MnO_2 (v.s.), Mn_2O_3 and/or Mn_3O_4 (tr.), La_2O_3 and $La(OH)_3$ (v.s.), Ag (s.)	13.3

[a] TAOH, tetraethylammonium hydroxide $(C_2H_5)_4NOH$, 35 wt% aqueous solution.
[b] Element contents determined by X-ray fluorescence spectroscopy (XRF).
[c] Phase composition determined by X-ray diffraction (XRD): s., small amount; v.s., very small amount; tr., traces.

X-ray photoelectron spectra of samples were taken in a commercial ultrahigh vacuum system, which consists of a fast entry specimen assembly, a preparation, and an analysis chamber. The analysis chamber is equipped with a hemispherical electron energy analyzer (SPECS LH-10), a twin anode X-ray gun for XPS, and a discharge lamp for UPS measurements. The base pressure was 5×10^{-10} mbar. The spectrometer was calibrated using the Fermi edge position of a sputter-cleaned Au foil, which was defined as binding energy (BE) zero of the spectra. Unmonochromatized Al-K_α line at 1486.6 eV and an analyzer pass energy of 97 eV, giving a full width at half-maximum (FWHM) of 1.7 eV for the Au $4f_{7/2}$ peak, were used in all XPS measurements. The electron binding energies were referenced to the Au $4f_{7/2}$ peak of the Au foil, at 84.00 ± 0.05 eV.

The samples were mounted on a steel holder and transferred to the main chamber in order to be characterized by XPS. All spectra were taken in normal emission and the measurements were performed under pressures less than 5×10^{-8} mbar. The XPS core-level spectra were analyzed with a fitting routine which decomposes each spectrum into individual, mixed Gaussian–Lorentzian peaks using a Shirley background subtraction over the energy range of the fit. The binding energies were calculated by reference to the energy of the C 1s peak of contaminant carbon at 285 eV. The surface composition of all the samples in terms of atomic ratios was calculated, using a Shirley-type background and empirical cross-section factors for XPS [33].

The temperature-programmed reduction of the catalysts was carried out in the apparatus AMI-1 (Altamira Instruments Inc.) using 0.05 g of catalyst placed in a flow quartz reactor with an internal diameter 7 mm. A 6% H_2–Ar mixture was used as carrier gas at a flow rate of 30 cm^3/min.; the linear temperature increase was 10 K/min. Immediately before reduction, the samples were dried in a stream of argon (30 cm^3/min.) at 373 K for 0.5 h and then cooled to room temperature. Water vapor formed during reduction was removed in a cold trap (immersed in liquid nitrogen–methanol slush) placed before the thermal conductivity detector (TCD). The TCD signal was calibrated by injecting 55 µl of argon to the carrier gas—the argon–hydrogen mixture.

The temperature-programmed oxygen desorption from the catalysts was performed with the apparatus AMI-1 coupled with a quadrupole mass spectrometer HAL 201 RC (Hiden Analytical). Catalyst samples weighing 0.2 g were placed in the quartz reactor. The pretreatment of the sample consisted of a heating ramp of 20 K/min to 1053 K in a mixture of 5% O_2/He with flow rate of 30 cm^3/min, followed by cooling to room temperature. The end pretreatment temperature was by 20 K lower than the calcination temperature for all catalysts; so such pretreatment did not change the characteristic of the catalysts. TPD of oxygen was performed with helium as carrier gas and a heating rate of 20 K/min up to 1173 K. The signal of the mass spectrometer corresponding to oxygen ($m/e = 32$) desorbed from the sample was recorded.

The methane–air mixture undergoes ignition when the methane content is above 5.3 vol% and then the adiabatic temperature rise is possible. In order to prevent an uncontrolled temperature rise and to keep the catalyst bed quasi-isothermal, experiments with flameless combustion performed at ambient pressure in the quartz reactor employed a methane–air mixture in which the methane concentration was 2 vol% and a small amount, 0.15 g, of powdered catalyst additionally diluted by mixing it with quartz at a ratio of 1:15. The reaction mixture was fed at a flow rate of 300 cm^3/min. The small amount of the catalyst, its very small grains, and the high space velocity of the oxygen-rich reaction mixture, equal to 120,000 $cm^3/(h\,g_{cat})$, minimized the external and internal mass and heat transport limitation. The reaction temperature was monitored by a chromel–alumel thermocouple inserted in the center of the catalytic bed. The initial examination of the reaction of methane ox-

idation demonstrated that quartz showed catalytic activity only at temperatures much higher than those at which complete combustion of methane in the presence of catalysts was obtained. The reaction temperature was increased step-by-step, until 100% methane conversion was achieved. After 20 min of stabilization at each temperature, analyses of the reaction products were conducted 3–4 times, and then results were averaged. The same procedure was applied during cooling of the catalyst starting from the temperature at which complete conversion of methane occurred. The reaction products, unreacted methane, and oxygen, were analyzed by gas chromatography, using an Alltech CTR1 column made of two coaxial columns—the inner column was packed with a porous polymer mixture, whereas the outer one contained an activated molecular sieve packing.

3. Results

3.1. Catalyst characterization

The XRD analysis (Fig. 1) showed that the main phase of the catalysts is an oxide system with a perovskite structure (Table 1). It was nonstoichiometric oxygen-excess $LaMnO_{3+\delta}$ with a rhombohedral–hexagonal structure (JCPDS 32-484), rather than orthorhombic, rigorously stoichiometric $LaMnO_3$ (JCPDS 33-713). Manganese oxides (Mn_2O_3 JCPDS 18-803, Mn_3O_4 JCPDS 24-734, MnO_2 JCPDS 18-802) and lanthanum oxide La_2O_3 (JCPDS 22-369 and 24-554) were also present. Their amounts were small for most catalysts. Since the samples were exposed in air before and during these analyses, the XRD patterns indicate the presence of phases of lanthanum hydroxide ($La(OH)_3$ (JCPDS 36-1481)) and lanthanum dioxycarbonate ($La_2O_2CO_3$ (JCPDS 23-320, 23-322, and 22-1127)). Their presence is justified by the basicity of lanthanum oxide, due to which it easily binds water vapor and carbon dioxide from air [34]. Hydroxyl compounds are readily removable by heating to 573 K and that is why during methane oxidation they should not be present in the catalysts. The carbonate phases decompose above 1070 K [35] and lanthanum dioxycarbonate is formed as an intermediate in the decomposition [34]. Its presence may then result from incomplete carbonate decomposition during calcination and from the fact that $La_2O_2CO_3$ decomposition is a reversible process in an atmosphere containing carbon dioxide [36]. In 0.1AgMnLa catalysts, precipitated with ammonium carbonate, the amounts of phases of lanthanum compounds and free manganese oxides, in comparison with the amounts of perovskite phase, were much higher than in the catalysts prepared with tetraethylammonium hydroxide. Relatively large amounts of lanthanum compounds unbound with the perovskite structure and free manganese oxides, Mn_2O_3 and/or Mn_3O_4, were present in 0.1AgMnLa-CD. Precise identification of these manganese oxides, whose amounts were still lower than those of lanthanum compounds, was difficult because of the overlapping of diffraction lines of various phases.

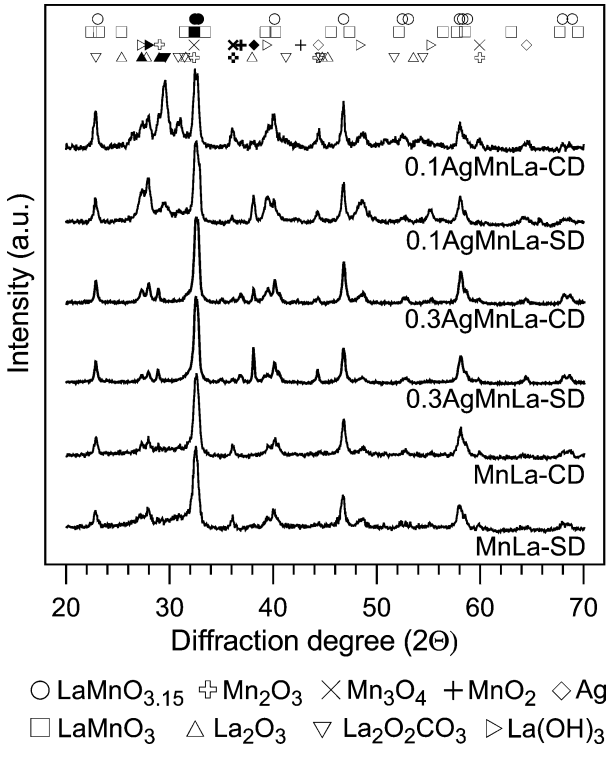

Fig. 1. XRD patterns of manganese–lanthanum catalysts. The diffraction lines characteristic of various phases are given at the top; the main lines are marked by filled symbols.

The bulk silver phase which can undoubtedly be observed in XRD patterns of catalysts 0.1AgMnLa and 0.3AgMnLa was metallic silver (JCPDS 4-783). Its amount depended on the drying method—higher diffraction peaks of silver are observable after supercritical drying of catalyst precursors. The great proximity of the strongest diffraction lines of silver ($2\theta = 38.16$), silver oxide Ag_2O ($2\theta = 32.78$ and 37.97 according to JCPDS 12-793), and perovskite ($2\theta = 32.59$ and 32.96) and weaker lines of manganese oxides and lanthanum compounds made it impossible to state unequivocally that bulk Ag_2O was present. Quite certainly the catalysts did not contain a Ag_2O phase in agreement with JCPDS 19-1155 (the strongest diffraction line at $2\theta = 38.62$). The absence of the bulk phase of silver oxide with the simultaneous presence of metallic silver is understandable, since the decomposition of Ag_2O to the metal occurs at temperatures of about 500–600 K [25,37], that is, at a temperature lower than that of catalyst calcination. Nor did the catalysts contain $AgMn_2O_4$ in agreement with JCPDS 16-740 or $Ag_2Mn_8O_{16}$ (JCPDS 29-1143). This does not necessarily imply absence of silver cations in the catalysts, which may be present in a separate, strongly dispersed phase of surface oxidized silver [32] or in the perovskite structure. The substitution of a small amount of lanthanum cations in the perovskite with another cation practically does not change its crystallographic structure [19,23,38–40].

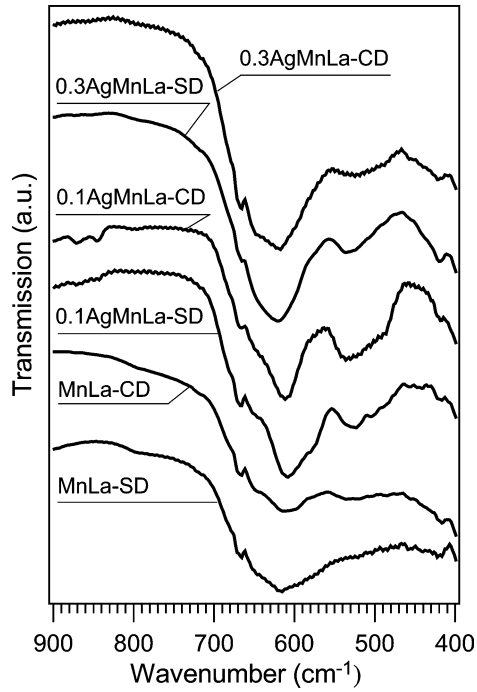

Fig. 2. Transmission FTIR spectra of manganese–lanthanum catalysts.

While phase identification can be obtained from X-ray diffraction data, FTIR spectroscopy can provide information on the local environments of metal cations in the oxide lattice and on the local lattice distortions. IR spectra of the catalysts are shown in Fig. 2. The spectra are dominated by an absorption band in the region 700–550 cm^{-1}, centered at 610–620 cm^{-1}. Other bands are visible at 550–470 cm^{-1} and below 470 cm^{-1}. It has been reported [41,42] that the IR spectrum of the lanthanum–manganese powder perovskite in the mean infrared region shows an evident band at 650–550 cm^{-1} (which arises from the asymmetric Mn–O–Mn stretching in the perfect octahedral species MnO_6, causing the internal motion of the manganese ion against the MnO_6 octahedron), bands at 480 cm^{-1} (weak), and at 395 cm^{-1}. The splitting of the higher frequency band (with two components at 608 and 570 cm^{-1} only partially resolved) and the low complexity of the region below 500 cm^{-1} was interpreted as being more in agreement with the rhombohedral oxygen-rich structure than with the orthorhombic stoichiometric phase. In the spectra of manganese–lanthanum catalysts (MnLa-SD and MnLa-CD) shown in Fig. 2, the main bands may be considered—also in agreement with the XRD results—as derived from the perovskite with an oxygen-rich structure. The broadening of the IR bands may indicate a random nonstoichiometry of the perovskite [42]. Since the perovskite structure cannot host interstitial oxygen, the defect chemistry of $LaMnO_{3+\delta}$ was described with randomly distributed La and Mn vacancies in equal amounts [43].

The structure of the perovskite is described as a sequence of MnO_6 octahedrons (linked through corners) with the La^{3+} ions located in 12-coordinated sites between the MnO_6 layers. Bands arising from the apical bonds in La–O (also Ag–O in silver-modified catalysts) occurring in the perovskite structure may be expected to appear in the far infrared region, i.e., in the low-frequency (below 400 cm^{-1}) region [41,44]. The spectra in Fig. 2 do not cover that infrared region. However, in the spectra of all catalysts there appears the broad vibrational absorption band at 550–470 cm^{-1}, more intensive at 540–530 cm^{-1}. Only in MnLa catalysts this is rather weak, especially in MnLa-SD. The modification of the catalysts with silver greatly increases the intensity of that band. Its presence in the spectra of unmodified catalysts excludes Ag_2O as its source. The band characteristic of this oxide should appear at 550 cm^{-1} [45]; therefore, it may be assumed that in none of the silver-containing catalysts the IR spectra showed the presence of pure Ag_2O. However, the considerable increase in the intensity of the bands at 550–470 cm^{-1} in the spectra of modified catalysts may indicate its connection with the presence of silver and the replacement of some lanthanum ions with silver ions in the perovskite structure. In silver-containing manganese–lanthanum oxide catalysts, when La^{3+} is substituted by Ag^{+} in the perovskite structure: (*i*) a large-size Ag^{+} ion with the lower oxidation state is incorporated in place of the smaller size La^{3+} ion, and (*ii*) Mn^{3+} ions are oxidized to the smaller Mn^{4+} ions. Mn^{3+} and Mn^{4+} ions in the rhombohedral and orthorhombic structure of perovskites can be arranged only in a disordered manner [46]. Consequences of the substitution of lanthanum ions also involve changes in the local symmetry of the MnO_6 units and the degree of distortion of the MnO_6 octahedrons. Deformations of the perfect oxygen octahedral construction with parallel axes of octahedrons are greater; they consist in the deflection of octahedrons from vertical positions and twists of octahedral chains. There emerges a distorted perovskite lattice. The result is a large variation in the local environment around manganese ions and the appearance of additional frequencies in the vibrational spectrum. The broad band at 550–470 cm^{-1} may be interpreted as originating from the bending vibration sensitive to octahedral distortion and to Mn–O–Mn bond angle modulations [44,47]. The intensities of the bending vibration band are smaller than those of the stretching vibrations associated with the Mn–O bond-distance variations. The rise in the intensity of the vibrational band at about 400 cm^{-1} (arising from external deformation of the MnO_6 octahedrons [44,47]) in the spectra of modified catalysts, in comparison with the unmodified ones, also indicates that silver ions have been incorporated in the perovskite structure.

The general broadness of our IR spectra and the evident, though weak, bands in positions other than those expected for the perovskite, may be associated with the presence of other phases. In positions 670, 600, 580, 530, 490, 450, and 410 cm^{-1}, IR bands arising from α-Mn_2O_3 were observed [48]. The IR bands of Mn_3O_4 occur at 610–620, 500, and 412–430 (weak) cm^{-1} [48,49], and of MnO_2 at 650–660, 600, and 520–530 cm^{-1} [48] or at 615 and 400 cm^{-1} [50]. The great proximity of the bands makes it difficult to distinguish manganese oxides in the IR spectra.

Additionally, many of these bands may be superimposed on bands characteristic of the perovskite in the catalysts of this work. However, the small peaks centered at around 670 and 415–420 cm^{-1} and the shoulder at 650 cm^{-1} may originate from the presence of small amounts of pure manganese oxides, found also in XRD patterns.

FTIR spectra did not show the presence of pure La_2O_3 in any of the catalysts—the band of this oxide should occur at around 450 cm^{-1} [51]. Nevertheless, there are probably small amounts of lanthanum hydroxide whose bands at 640–647 cm^{-1} [51,52], characteristic of bending OH vibrations, are poorly marked in IR spectra. It is an effect of the contact of the surface of the samples with air. In catalyst 0.1AgMnLa-CD, in positions around 845 and 870 cm^{-1}, there are clearly marked bands (with lower intensity also in 0.1AgMnLa-SD) derived respectively from the carbonate group in $La_2O_2CO_3$ and an unidentately bound carbonate species [34,52]. This is in agreement with the XRD results, which reveal the presence of a fraction of lanthanum not involved in the perovskite structure in catalysts precipitated with ammonium carbonate.

The characterization of chemical species located in the near-surface region of the catalysts was carried out by XPS and the results are summarized in Table 2. The O 1s spectra exhibit two features, which are shown in Fig. 3. The peak at lower binding energy, 529.4–529.8 eV, corresponds to lattice oxygen (O^{2-}), whereas the one at 531.25–531.8 eV corresponds to several O ls states assigned to the surface-adsorbed oxygen such as O_2^{2-} or O^-, in the form of hydroxyl OH^- and carbonate CO_3^{2-} species (all fall in the 531–532 eV range) as well as associated with adsorbed molecular water (above 533.0 eV) [23,39,53–56]. In catalysts precipitated with TAOH the participation of surface-adsorbed oxygen species, probably mostly hydroxyls, was the same and it equaled about 60% of the total amount of oxygen, whereas in catalysts precipitated with ammonium carbonate it was much greater—about 76% in the case of 0.1AgMnLa-CD and about 82% in that of 0.1AgMnLa-SD. Such an increased participation of $O_{surface}$ in catalysts precipitated with ammonium carbonate certainly results from the presence of greater amounts of carbonate groups, confirming the results of XRD and FTIR. The method of precursor drying does not affect the distribution of the oxygen species in the surface layer of the catalysts. The low values of the ratio $O_{lattice}$/Mn may imply the presence of lattice vacancies of O^{2-} ions on the catalysts surface, eventually filled up with adsorbed, weakly held (i.e., in comparison with O^{2-} ions) oxygen species and/or surface hydroxyl and carbonate groups. An alternative may be the presence of coordinatively unsaturated surface ions of manganese in all the catalysts. As has been noted earlier, when discussing XRD results, adsorbed oxygen and hydroxyl groups are readily removable. The carbonate species are harder to remove and during methane oxidation they may remain on the surface of the catalysts.

The binding energy values of La $3d_{3/2}$ and La $3d_{5/2}$ (the spin–orbit splitting of La was 16.8 eV) were almost constant for all the catalysts (Fig. 3) and were close to values characteristic of pure lanthanum oxide, i.e., 834.4 for La $3d_{3/2}$ and 837.8 eV for La $3d_{5/2}$ [53,54]. Small variations were ascribed to changes in the crystal structure and/or electronic structure. In Ref. [57] the La $3d_{5/2}$ spectrum of the $LaMnO_{3+\delta}$ was deconvoluted to four peaks. The peak at 833.7 eV (in [58] at 833.9 eV) was attributed to La^{3+} of the perovskite and the signal at 835.7 eV to the La^{3+} of lan-

Table 2
La 3d, Mn 2p, Ag 3d, and O 1s binding energies (C 1s at 285 eV)

Catalyst	La 3d (eV)	Mn 2p (eV)	Ag 3d (eV)	O 1s (eV)	Mn^{4+}/Mn^{3+}	La/Mn	(La + Ag)/Mn	Ag/Mn	Ag/La	O_{total}/Mn	$O_{lattice}$/Mn
MnLa-CD	834.35 838	641.45 643 645		529.65 531.25	0.746	0.278	0.278			2.06	0.834
MnLa-SD	834.6 838.2	641.6 643.2 645.1		529.8 531.6	0.909	0.334	0.334			2.36	0.93
0.1AgMnLa-CD	834.65 838.32	641.47 642.93 644.84	368.25 374.25	529.6 531.75	1.11	0.467	0.574	0.107	0.174	3.03	0.718
0.1AgMnLa-SD	834.15 837.8	641.5 643.5 646	368.25 374.25	529.4 531.8	1.13	0.478	0.617	0.139	0.29	3.36	0.614
0.3AgMnLa-CD	834.32 838	641.6 643 644.8	368.3 374.3	529.75 531.75	1.16	0.291	0.453	0.162	0.559	2.48	0.992
0.3AgMnLa-SD	834.3 837.9	641.5 642.85 644.8	368.3 374.3	529.55 531.4	1.06	0.338	0.527	0.189	0.558	2.54	1.02

The surface composition of samples is presented in terms of atomic ratios.

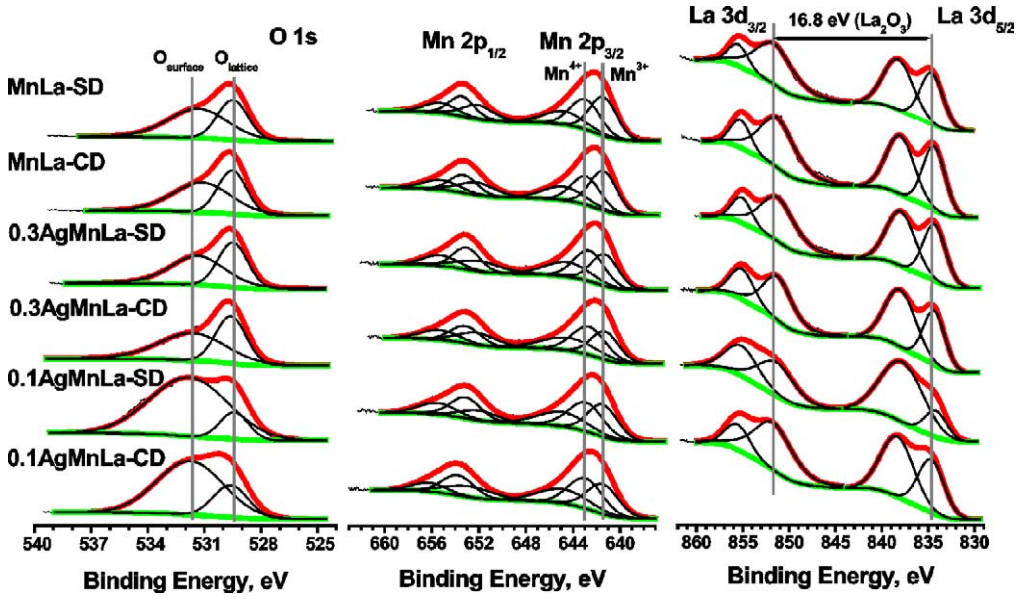

Fig. 3. XPS spectra for O 1s, Mn 2p, and La 3d of manganese–lanthanum catalysts.

thanum surface carbonate [57,58]. The peaks at 837.8 and 839.0 eV were interpreted as due to the strong screening effect of f electrons of the two first La^{3+} features [57]. The present La $3d_{5/2}$ spectra undoubtedly indicate that lanthanum ions in trivalent form, without any neighboring oxygen vacancies, occur on the surface of all the catalysts. However, they are fewer than in the bulk of the catalysts, which is indicated by the values of the ratios La/Mn and Ag/La, also shown in Table 2. The ratio La/Mn in samples dried with supercritical carbon dioxide during preparation is greater than in samples dried conventionally.

The binding energies of Mn $2p_{3/2}$ and Mn $2p_{1/2}$ (Table 2) are very similar to those reported in the literature [23,54]. Since the differences between the binding energy values of Mn^{3+} and Mn^{4+} ions are small, a peak synthesis procedure, which includes three components—Mn^{3+}, Mn^{4+}, and a satellite [23,54]—was applied. The fitted XPS spectra of Mn 2p are shown in Fig. 3. The component at 641.4–641.6 eV is attributed to Mn^{3+} and that at 642.8–643.5 eV to Mn^{4+} ions [23]. The value of the Mn^{4+}/Mn^{3+} ratio (Table 2) in the surface layer of MnLa catalysts was quite high (0.75–0.9) and still increased to about 1.1 in modified catalysts—the presence of silver enforced the transformation of a larger amount of Mn^{3+} ions to Mn^{4+} ions. In order to check for the possibility of surface reduction during the XPS measurements, the Mn 2p peak was recorded both in the beginning and in the end of the measurements (i.e., after prolonged irradiation time) and no change in the shape or intensity of the Mn 2p peak was found. The transformation of a larger amount of Mn^{3+} ions to Mn^{4+} ions in the presence of silver is caused by the fact that charge compensation in $LaMnO_{3+\delta}$ after the substitution of some lanthanum ions with silver ions may be achieved by manganese oxidation and by oxygen loss with eventual appearance of oxygen vacancies. No significant differences in the values of the ratio Mn^{4+}/Mn^{3+} in modified catalysts were observed, despite different amounts of silver in their bulk phase. Varied parameters of the preparation, i.e., both the kind of the precipitating agent and the method of precursor drying, had no unequivocal influence on the mutual ratios of both kinds of manganese ions in the surface layer of the catalysts.

Analysis of the values of La/Mn and (La + Ag)/Mn ratios indicates that the surface of all catalysts has been significantly enriched with manganese. In the surface layer of unmodified catalysts manganese ions are about three times more numerous in relation to lanthanum ions than in the bulk phase. In silver-containing catalysts, in which the bulk La/Mn ratio was about 0.9 or 0.7, the migration of manganese ions toward the surface is smaller, but their amount in the surface layer is still about two times greater. The degree of manganese segregation (1.6–2.2 times higher) is similar also in relation to the sum of lanthanum and silver. Supercritical drying facilitated the preparation of materials in which manganese enrichment of the surface was somewhat smaller than after conventional drying. Manganese enrichment of the surface of manganese–lanthanum perovskites was reported in [23], but migration of lanthanum toward the surface has been also observed [54,58]. Our results confirm the findings of the former report.

The XPS spectra for Ag 3d and the Auger MNN spectra of the manganese–lanthanum catalysts modified with silver are shown in Fig. 4. The binding energies of Ag $3d_{5/2}$ and Ag $3d_{3/2}$ (Table 2) may be interpreted as corresponding to metallic silver. According to literature data, the binding energy of Ag $3d_{5/2}$ for metallic silver is 368.3 eV, 367.5 eV for Ag_2O, and 367.3 eV for AgO [28]. On the surface of the catalysts modified with silver there are no silver ions derived from pure silver oxides, which is in agreement with the results of XRD and FTIR, where such phases were not detected. We also examined the kinetic en-

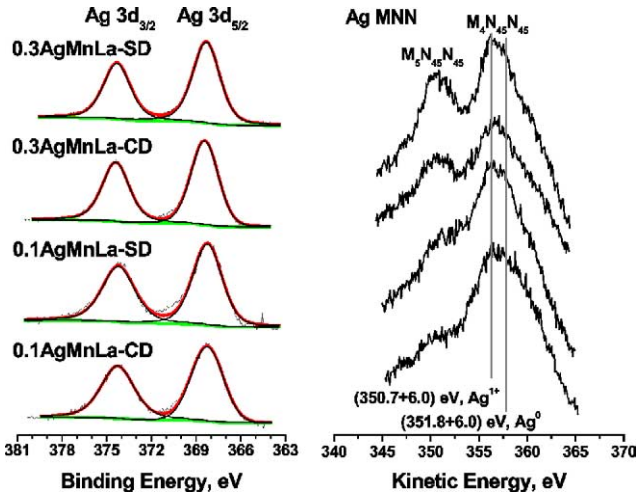

Fig. 4. XPS spectra for Ag 3d and Auger MNN spectra of manganese–lanthanum catalysts modified with silver.

ergy of the Ag NMM Auger electrons emitted from silver-containing catalysts (Fig. 4). However, there appears a difficulty, because the Auger line of silver is very close to the XPS line of lanthanum; nevertheless, the kinetic energy of the Auger $M_4N_{45}N_{45}$ peak is closer to the kinetic energy of Ag^+ (356.6 eV) than the kinetic energy of Ag^0 (358.1 eV) [32]. The calculated Auger parameters (Auger parameter = Ag $3d_{5/2}$ + ($M_5N_{45}N_{45}$ + 6 eV)) for the catalysts were equal to 725.2 eV in the case of 0.1AgMnLa-CD, 725.0 eV for 0.1AgMnLa-SD, and 724.65 eV for both 0.3AnMnLa-CD and 0.3AgMnLa-SD. Because in the literature [33] the Auger parameter reported for metallic silver Ag^0 is 725.8–726.3 eV and for Ag^+ ions 724.5 eV, it appears that most of silver in the near-surface region of the silver-containing catalysts is present as partially oxidized, i.e., as Ag^+ ions. In Ref. [32] such a situation was interpreted as the oxide-covered or the oxygen-covered surface of metallic silver particles (which were supported on zirconia). Since the XRD experiments of modified catalysts showed the presence of a separate phase of metallic silver, one may suppose that this is also covered with an oxygen-containing layer and the presence of strongly dispersed Ag_2O, invisible in the XRD, is also possible. In manganese–lanthanum oxides modified with silver the Ag^+ ions should also occur in the perovskite structure.

The values of the ratio Ag/Mn did not indicate the enrichment of the surface layer of modified catalysts with silver; in the case of 0.3AgMnLa it was even poorer with silver than their bulk. On the other hand, the mutual ratios of silver and lanthanum (Ag/La) were in each case higher than in the bulk of the catalysts, which is certainly a result of the lanthanum depletion of their surface. The chemical composition of the near-surface region of the catalysts in comparison with their bulk phase is shown in Table 3.

Experiments of the reducibility of the catalysts have shown (Fig. 5) that their reduction occurs in two regions: a low-temperature region, up to about 800 K, and a high-

Table 3
Surface[a] and bulk[b] (in brackets) composition of the manganese–lanthanum catalysts in terms of atomic ratios

Catalyst	Mn (at%)	La (at%)	Ag (at%)	O (at%)
MnLa-CD	30.0 (17.4)	8.3 (18.6)		61.7 (65.0)
MnLa-SD	27.0 (17.1)	8.3 (18.8)		64.7 (64.0)
0.1AgMnLa-CD	21.7 (16.1)	10.0 (14.6)	2.2 (2.1)	66.1 (67.1)
0.1AgMnLa-SD	20.0 (17.4)	9.6 (16.6)	2.8 (2.3)	67.6 (63.7)
0.3AgMnLa-CD	25.4 (15.7)	7.4 (11.3)	4.2 (5.1)	63.0 (68.0)
0.3AgMnLa-SD	24.5 (16.8)	8.3 (12.3)	4.7 (5.7)	62.5 (65.1)

[a] Surface element contents determined by X-ray photoelectron spectroscopy (XPS).
[b] Bulk element contents determined by X-ray fluorescence spectroscopy (XRF).

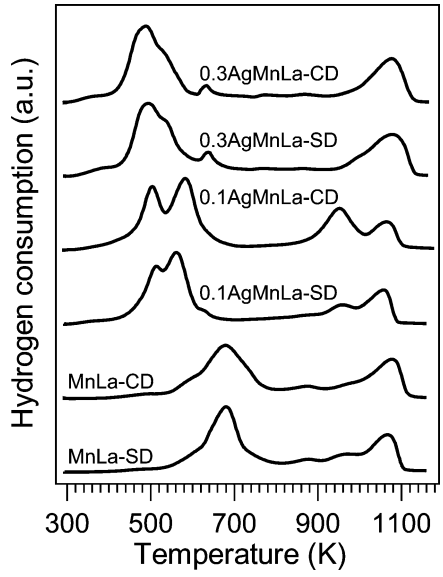

Fig. 5. H_2-TPD profiles of manganese–lanthanum catalysts.

temperature region up to 1100–1130 K. Two major peaks during temperature-programmed reduction of lanthanum–manganese perovskites have been observed previously [13,17,59]—the first phase of the reduction was interpreted as the reduction of Mn^{4+} to Mn^{3+}, while the other was ascribed to the reduction of Mn^{3+} to Mn^{2+} with concomitant destruction of the perovskite structure. In the case of MnLa catalysts, the reduction begins at about 540 K and the maximum rate of the low-temperature stage of the reduction occurs at about 670–680 K. The shoulder at the lowest temperature, of about 590 K, was interpreted in [23] as the removal of nonstoichiometric excess oxygen, which is most weakly bound in the perovskite lattice. The second shoulder, at temperatures above those of the first peak, may be a result of the overlapping of the reduction peaks of perovskite and of small amounts of free manganese oxides or those containing small amounts of lanthanum ions in their crystal lattice. It has been reported in [60] that in the temperature range in which the first stage of reduction takes place, there occurs complete reduction of nonsupported MnO_2 to MnO and the beginning of Mn_2O_3 reduction; in Ref. [61] they also ob-

served peaks of the reduction of Mn_3O_4, while in Ref. [30] complete reduction of Mn_2O_3 to MnO was observed. Small peaks at about 875 and 970 K may also derive from the reduction of manganese oxides, which are not incorporated in the perovskite structure. The maximum of the rate of the second stage of perovskite reduction occurs at 1070–1080 K.

The presence of silver in the catalyst considerably lowers the temperature of the first stage of reduction, even by almost 200 K. The facilitation of the reduction is greater, the more silver there is in the catalyst. A similarly large lowering of the reduction temperature was observed in the case of complex manganese–silver oxides [29,30] and $Ag–Mn/Al_2O_3$ catalysts [27], and the temperature of the beginning of the reduction of binary oxides was close to that of the reduction of systems containing only silver. The promotion of the reduction of manganese-containing oxides is sometimes accounted for by the activation and then the spillover of hydrogen from metallic silver, formed already during the calcination stage. Another explanation was offered in Refs. [62,63] which suggest that the presence of metals from the copper family (Cu, Ag, Au) leads to a weakening of the strength of the metal–oxygen bonds in the main oxide being reduced, located near the coinage metal. It may be expected that in a similar way silver facilitates the pulling out of oxygen from the crystal lattice of the oxides in the present case. The structural defects induced by silver may also increase lattice oxygen mobility in the catalysts. Thanks to the weakening of the bonds between oxide and manganese ions, the migration of lattice oxygen to metallic silver becomes probable. Since the release of oxygen from silver oxides (reduction at a relatively low temperature, and even their spontaneous thermal decomposition) is easier than in the case of manganese oxide compounds, then the sequence of events—the weakening of the bonds Mn–O, increased lattice oxygen mobility and its migration to silver—results in the lowering of the temperature necessary for the first stage of the reduction of modified catalysts. Naturally, this is possible only after the introduction of silver ions into the structure of manganese oxide (perovskite) or after bringing about a very intimate contact of silver and manganese phases in some other way.

Similarly to MnLa catalysts, additional reduction peaks in silver-modified catalysts are complex and their interpretation is even more complicated. There is an additional factor to be taken into account—the extent of direct contact of oxides being reduced with silver. The small peaks of reduction at 635 K probably originate from the reduction of unmodified perovskite or manganese oxides. In the profiles of temperature-programmed reduction of catalysts 0.1AgMnLa, precipitated by ammonium carbonate, the number and intensity of peaks in temperature ranges characteristic of both low- and high-temperature reduction regions are greater than for the remaining catalysts. This undoubtedly results from the great nonhomogeneity of these catalysts (which is indicated in the analysis of XRD patterns and FTIR spectra) and the probable coexistence of two phases of manganese–lanthanum composite oxides, with low lanthanum oxide content (easier to reduce) and with the perovskite structure (harder to reduce). The XRD results of the catalysts indicated the existence of lanthanum compounds not bound in the perovskite structure in catalysts 0.1AgMnLa.

The temperature range in which the high-temperature stage of perovskite reduction takes place is similar for all catalysts, irrespective of whether they contain silver or not.

The total amount of hydrogen utilized for the reduction of the oxide phase in silver-modified catalysts is somewhat larger (2.54–2.76 mmol/g) than in the case of catalysts MnLa (2.14–2.18 mmol/g). Yet there seems to be no systematic dependence on the silver content in the catalyst or on the manner of the preparation (kind of the precipitating agent, drying method). An increase in the amount of utilized hydrogen is evidenced mainly in the low-temperature region of the reduction. In the temperature range above 770 K the utilization of hydrogen for all the catalysts shows only small differences, ranging from 0.94 to 1.16 mmol/g. Such a temperature distribution of the amounts of utilized hydrogen may indicate a larger amount of easily removable oxygen and a higher content of Mn^{4+} ions in the modified catalysts. Equally evident is also its small dependence on silver content. This is in agreement with the XPS results (Table 2) and it supports the conclusion regarding the increased value of the Mn^{4+}/Mn^{3+} ratio in modified catalysts, also in their bulk phase.

O_2-TPD experiments for manganese–lanthanum catalysts showed the existence of three temperature ranges of desorption (Fig. 6). The low-temperature desorption peaks (in the range of 500–700 K, with maxima at 550–560 K in the

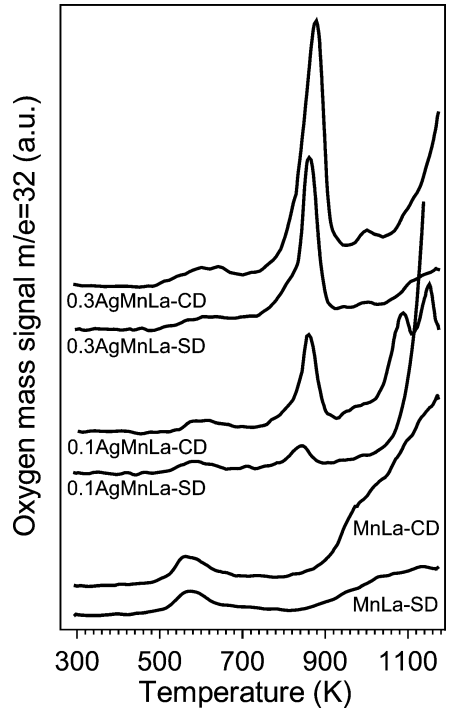

Fig. 6. O_2-TPD profiles of manganese–lanthanum catalysts.

case of MnLa and at about 590 and 610 K for 0.1AgMnLa and 0.3AgMnLa, respectively) are ascribed [13,64] to the weakest, molecularly adsorbed (suprafacial) oxygen on the surface of the catalysts. The desorption of the second kind of oxygen from MnLa catalysts begins very slowly at about 850 K and continues at higher temperatures. It is oxygen originating from the crystal lattice of oxides (intrafacial oxygen)—nonstoichiometric and connected with the reduction of Mn^{4+} to Mn^{3+}, as suggested in Refs. [12,13,23,39,64,65]. In the presence of silver there appears a third peak of oxygen desorption (most probably also intrafacial) with the maximum at about 840–870 K. The size of this additional peak of oxygen desorption is inversely proportional to the intensity of diffraction lines of metallic silver observed in XRD spectra. It suggests that this kind of oxygen probably does not derive from large crystallites of metallic silver, observed in X-ray diffraction. This suggestion seems to be confirmed by the results of Ref. [66] in which two different forms of subsurface atomic oxygen in metallic silver were identified—the bulk-dissolved (O_β) and oxygen (O_γ) which substitutes silver atoms in the lattice. The latter form of oxygen is located only in the uppermost silver layer. The temperature of O_β desorption was lower (a maximum below 760 K) and the thermal desorption of O_γ oxygen occurred at higher temperatures (a maximum above 950 K) than those at which desorption was observed in our silver-containing catalysts. In Ref. [24] the desorption of lattice oxygen from an unsupported silver oxide Ag_2O was observed at about 650 K, i.e., at a temperature much lower than that at which there occurs the additional peak of oxygen desorption, characteristic of our silver-containing catalysts. However, the temperature range of this additional peak of oxygen desorption is close to temperatures characteristic of oxygen desorption from silver catalysts and manganese–silver catalysts supported on Al_2O_3 [27] and from unsupported oxide catalysts Mn/Ag (80/20) and Mn/Ag/Sm (80/20/5) [31]. In Ref. [27] the peaks at 850–920 K were ascribed to the overlap between desorption of the lattice oxygen of MnO_2 and dispersed Ag_2O. The oxygen desorbed at 730 and 920 K from the manganese–silver unsupported oxides was interpreted as originating from the lattice of Ag_2O and Mn_2O_3 [31]. The temperature of oxygen desorption from manganese oxide in the composite catalysts was more than 200 K lower than that at which pure Mn_2O_3 released its oxygen. The above facts prove that the oxygen desorbed at 840–870 K from our silver-containing catalysts is derived from manganese–silver phases in which both components are in very close contact, such that silver ions are homogeneously dispersed in manganese oxides, as it happens in silver-substituted perovskites. In the presence of silver ions in the perovskite structure the lattice oxygen neighboring with them becomes thus much more labile (greater lability of the lattice oxygen was suggested also in the case of composite manganese–silver oxides [24,31]), probably due to the weakening of Mn–O bonds, and is desorbed at a lower temperature. This conclusion is further supported by the fact that the desorption of the remaining lattice oxygen, not activated by silver, begins at temperatures higher by about 200 K than in the case of catalysts MnLa. Unfortunately, the interpretation of the curves of oxygen desorption above 1050 K may contain errors caused by carbonate decomposition beginning at this temperature [35] and fragmentation of released carbon dioxide in the mass spectrometer. Nevertheless, the high-temperature part of the TPD profile of the 0.1AgMnLa-CD catalyst, obtained by precipitation with ammonium carbonate and dried conventionally, again implies its considerable nonhomogeneity.

3.2. Performance in methane oxidation

Carbon dioxide and water were the sole reaction products of methane oxidation; therefore, there was no carbon monoxide formed. The amount of carbon present in the form of carbon dioxide produced was equal to that in methane converted. The course of methane combustion (Fig. 7) on all the catalysts was similar, and all the catalysts followed the same temperature profile during heating up to achieve 100% methane conversion and then during cooling. On cat-

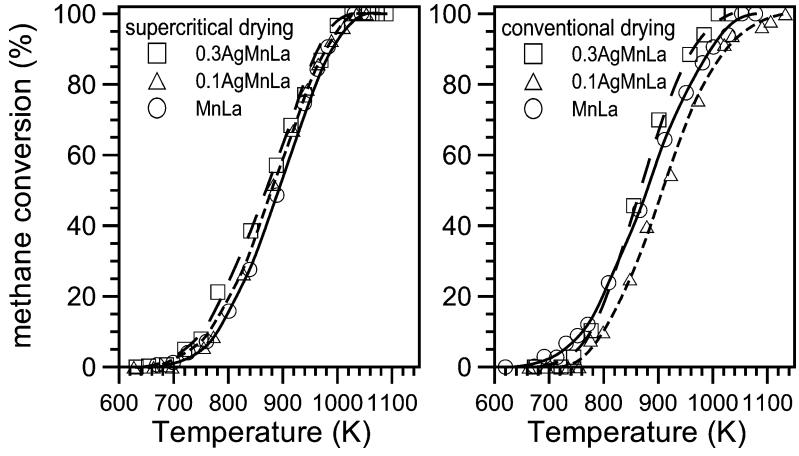

Fig. 7. Catalytic combustion of methane over manganese–lanthanum oxides modified with silver.

alysts dried with supercritical carbon dioxide the reaction began at about 680 K and unreacted methane totally disappeared above 1020 K. The introduction of silver into the composition of the catalyst from this group increased its activity, but only slightly. The beginning and end of methane combustion on catalyst MnLa dried in a conventional way occurred at temperatures similar to those in the case of the catalyst dried supercritically. Silver modification of the thus prepared catalyst caused a decrease of its activity at lower temperatures. At higher temperatures methane conversion on 0.3AgMnLa-CD exceeded the values obtained on unmodified MnLa-CD. The differences between temperatures necessary for the combustion of 10, 50, and 90% of methane on all the catalysts were not great (Fig. 8). Only on 0.1AgMnLa-CD were the values of these temperatures higher than those of the remaining catalysts. One may say that, on the whole, the preparation method and the presence of silver in manganese–lanthanum oxide catalysts had no significant influence on the temperatures at which flameless methane combustion began and methane complete combustion was accomplished. The temperature necessary to ignite the reaction was very close to that for MnO_x/Al_2O_3 catalyst, but almost 200 K lower than the temperature at which oxidation of methane began on La_2O_3/Al_2O_3 [8]. The positive effect of silver modification of manganese–lanthanum oxide catalysts in our experiments is by no means so obvious as indicated in Ref. [21] where a substitution of 30% of lanthanum with silver in manganese–lanthanum perovskite lowered the temperature of methane combustion by about 40 K.

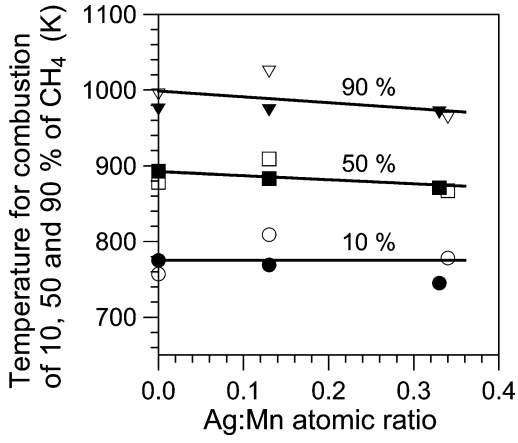

Fig. 8. Effect of the Ag:Mn atomic ratio on the temperature needed for 10, 50, and 90% conversion of methane (open symbols, conventional drying, CD; filled symbols, supercritical drying, SD).

Yet, the observed course of methane combustion is a function not only of the catalyst composition but also of its surface area. Taking into account the differences in the surface areas of the catalysts (Table 1), it appears that their modification with silver causes an increase in the rate of methane combustion (Fig. 9). An increase in the activity per unit of surface area for silver-containing catalysts in the temperature range of 770–870 K, where the degree of methane conversion is from 6 to 50%, is greater, the higher the reaction temperature. At higher temperatures in this range smaller amounts of silver were sufficient to increase the rate of the reaction—the differences between the rates of combustion on catalysts 0.1AgMnLa and 0.3AgMnLa are rather small.

The apparent energies of activation calculated from Arrhenius plots for silver-containing catalysts were not very different from the activation energies observed in the case of unmodified catalysts (Fig. 9). This suggests that the presence of silver does not change the reaction mechanism; the increase in the reaction rate results rather from a higher number of active sites involved in the reaction or from their higher specific activity.

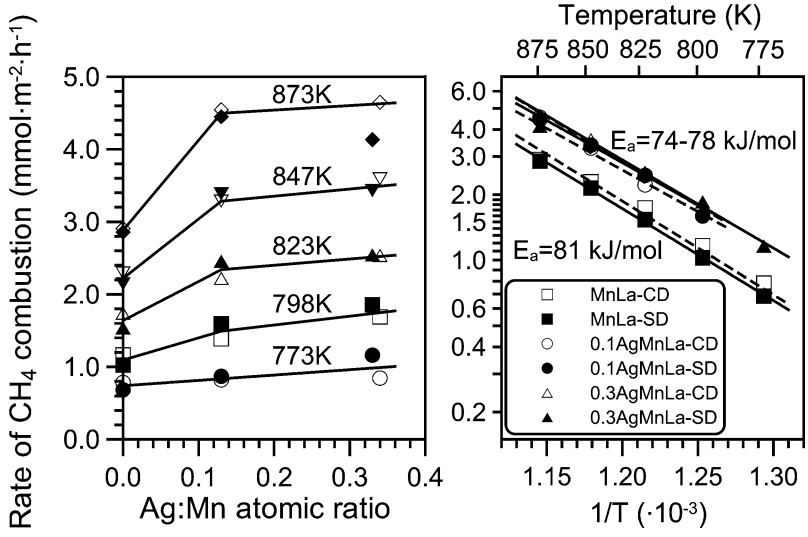

Fig. 9. Effect of the Ag:Mn atomic ratio on the rate of flameless combustion of methane (open symbols, conventional drying, CD; filled symbols, supercritical drying, SD).

4. Discussion

The manganese–lanthanum oxides modified with silver turned out to be a complicated multiphase catalytic system with the dominance of the perovskite phase. More uniform materials were obtained from precipitation with hydroxides than by precipitation with ammonium carbonate. The higher temperatures of the decomposition of carbonates compared to hydroxides, and the especially high temperature of lanthanum dioxycarbonate decomposition, make the reactions between manganese and lanthanum oxide phases during calcination more difficult and not all lanthanum enters the perovskite structure. The preparation of a more homogeneous phase composition of the oxides is facilitated by drying the precipitates with supercritical carbon dioxide. Due to the inhibition of the agglomeration processes of precipitated particles in this case, subsequent reactions between them during calcination are easier and quicker. The greater surface area of the contact of small particles of particular oxides facilitated the formation of the lanthanum–manganese perovskite structure.

Only a part of silver introduced into the catalysts was accommodated by the perovskite phase. In this case, the supercritical drying of the precipitate favored a part of metallic silver to remain as a separate phase. The cause of this could be the lack of aggregation of precipitate particles with silver oxide remaining in the form of separate particles. Silver oxide undergoes thermal decomposition already at about 500–600 K [25,37]. The absence of close contact with the particles of the other oxides could render their reaction with metallic silver more difficult than in the case when silver, still in the form of (hydro)oxide already at the beginning of calcination, was occluded in larger aggregates of the precipitate particles. The IR spectra of modified catalysts prove that part of the silver oxides was nevertheless incorporated into the perovskite structure, also after supercritical drying.

Differences in the preparation modes of the catalysts and their uniformity had only a small influence on their properties in the reaction of flameless methane combustion. The amounts of all kinds of cations in the near-surface region of the catalysts, which is most significant for the course of the catalyzed reaction, practically did not depend on the manner of preparation. The surface of all the catalysts was enriched with manganese ions in relation to the bulk of the solid and the surface amount of silver was similar to that in the bulk of the oxides.

O_2-TPD experiments showed that the modification of manganese–lanthanum oxides with silver provides a new source of oxygen, more weakly bound in the oxide structure. Due to the high stability of the perovskite structure, substitution of lanthanum cations with silver cations should create structural defects, i.e., there should emerge oxygen vacancies, which may be accompanied by a change in the balance between the transitional stages of manganese oxidation. These vacancies may be occupied by weakly held oxygen species under an oxygen-containing atmosphere, as

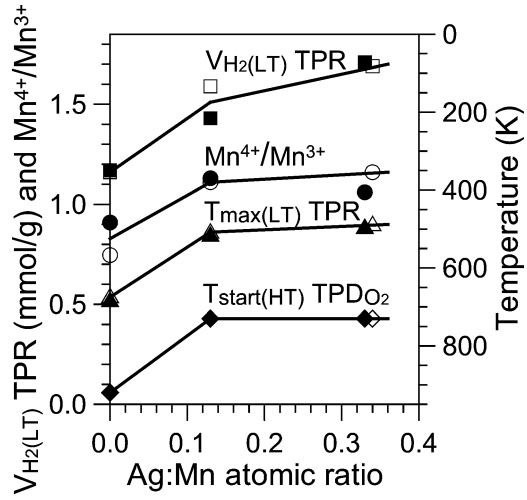

Fig. 10. Effect of the Ag:Mn atomic ratio on the Mn^{4+}/Mn^{3+} surface atomic ratio, amount of hydrogen consumed in the low-temperature region of the reduction ($V_{H_2(LT)}$ TPR), the temperature of the maximum of the low-temperature peak of the reduction ($T_{max(LT)}$ TPR), and the temperature of the start of the high-temperature peak of the oxygen desorption ($T_{start(HT)}$ TPD_{O_2}) (open symbols, conventional drying, CD; filled symbols, supercritical drying, SD).

compared to lattice oxide ions. These oxygen species, filling the vacancies, may be responsible for the easier and faster reaction with methane during its flameless combustion on modified catalysts. A comparison of Figs. 9 and 10 indicates that the temperature at which the high-temperature peak of oxygen desorption starts ($T_{start(HT)}$ TPD_{O_2}) depends on the Ag:Mn atomic ratio in a way similar to the rate of methane oxidation. The more weakly bound oxygen in silver-containing catalysts is more mobile and it may leave the catalyst surface more easily—it is therefore more readily available for methane oxidation. The binding strength of such oxygen species on the catalyst and the possibility of more facile desorption at lower temperatures (Figs. 6 and 10) are significant for catalyst activity. A considerable increase in the rate of reaction of methane with oxygen after introducing silver into the catalyst occurred only at higher temperatures, at which the participation of oxygen released from the crystal lattice or its filled up oxygen vacancies becomes possible.

The weakening of oxygen binding in silver-modified catalysts and the importance of the ease of removing it from the catalysts for the rate of methane oxidation are also indicated by the TPR results. The rate of methane combustion after the introduction of silver (Fig. 9) changes in a way similar to that of the temperature of the low-temperature peak of reduction ($T_{max(LT)}$ TPR) (Fig. 10).

It seems that for an increase in the rate of methane combustion large amounts of weakly bound oxygen are not necessary. The amount of hydrogen consumed in the low-temperature region of reduction ($V_{H_2(LT)}$ TPR), which is a measure of the amount of oxygen removed from the catalyst in this temperature range, also increases after catalyst modification (Fig. 10). Yet, although an increase of the

Ag:Mn atomic ratio from 0.1 to 0.3 further increased the amount of consumed hydrogen, this did not cause an equivalent increase in the rate of methane combustion (Fig. 9). The smaller importance of a large amount of weakly bound oxygen compared to the degree of bond weakening in the catalyst is also indicated by the different sizes of the high-temperature peak of oxygen desorption (Fig. 6)—the different size of these peaks has no direct relation with catalyst activity.

The effect on the rate of methane combustion following introduction of increasing amounts of silver into the catalyst (Fig. 9) is analogous to that on the surface Mn^{4+}/Mn^{3+} atomic ratios (Fig. 10). Partial substitution of lanthanum in the perovskite structure can induce oxygen nonstoichiometry. Still, the filling of oxygen vacancies must result in the appearance of a larger number of manganese ions in the unstable oxidation state Mn^{4+}. The value of the Mn^{4+}/Mn^{3+} surface ratio may therefore be considered as a significant parameter characterizing the intrinsic properties of manganese–lanthanum oxides (and probably also of other systems containing manganese oxides) which affects their activity in flameless combustion of methane. Fig. 11 shows that the rate of methane oxidation is a linear function of the Mn^{4+}/Mn^{3+} surface atomic ratio. Our results suggest that significantly larger amounts of Mn^{4+} ions are connected with the greater accessibility of oxygen for methane oxidation.

The oxidation reactions on perovskites have been characterized as suprafacial or intrafacial [10]. The suprafacial process, which proceeds at a low temperature, involves weakly bound oxygen species adsorbed on the catalyst surface. The low-temperature desorption of oxygen, most weakly bound with the catalyst surface, occurred at temperatures lower than those at which the reaction of flameless methane combustion began. The introduction of silver into the catalysts did not change its amount and binding strength in any significant way. Therefore, this oxygen species is not responsible for the specific activity of the modified catalysts. The intrafacial process, occurring at higher temperatures, involves lattice oxygen as an active species. Our results indicate that the flameless combustion of methane over manganese–lanthanum oxides is an intrafacial process. In the first stages of the reaction a metal oxide or only its surface is reduced by methane and then, on successive stages, the reduced metal oxide is again oxidized by oxygen adsorbed from the gas phase. The weakening of Mn–O bonds, facilitating the release of oxygen from the near-surface region of the catalyst layer, accelerates the reaction of methane oxidation. This conclusion is supported by the results reported in [20], which demonstrate that the introduction of silver into the structure $LaCoO_3$ increases the reactivity of the lattice oxygen during methane reaction, even in the absence of gaseous oxygen.

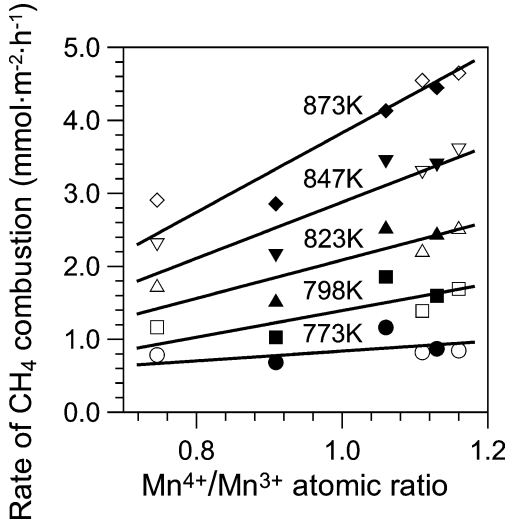

Fig. 11. Rate of flameless combustion of methane as a function of the Mn^{4+}/Mn^{3+} surface atomic ratio (open symbols, conventional drying, CD; filled symbols, supercritical drying, SD).

The fact of the weaker binding of oxygen with silver ions (reduction at a relatively low temperature and even spontaneous thermal decomposition of silver compounds) than with manganese ions is of great significance for the localization of the sites of methane oxidation (filled oxygen vacancies) on the surface of silver-modified catalysts. During the reaction, the oxygen neighboring with silver ions, which is bound more weakly than the oxygen neighboring only with manganese ions, should be utilized first for methane oxidation. The remaining part of the catalyst structure in which oxygen is bound only with manganese ions may constitute a specific reservoir of oxygen ions with which the vacancies are filled up—the flow of oxygen in the perovskite, where silver and manganese ions are in a common crystal lattice, should be even easier than through the contact site of two separate phases of manganese and silver oxides. The easiness of the flow of oxygen from manganese oxide to palladium was reported in Ref. [67] and from manganese oxide to copper in Ref. [68]. In turn, oxygen from the gaseous phase is first introduced in the neighborhood of easily oxidized manganese ions, thus filling up oxygen vacancies in the crystal lattice of the perovskite (or of manganese oxide). A similar mechanism of the oxidation of carbon monoxide and methane on manganese–silver composite oxides was proposed in Refs. [24,30,31].

5. Conclusions

Manganese–lanthanum oxides modified with silver constitute a complicated multiphase catalytic systems with the dominance of the perovskite phase. The precipitation of catalyst precursors with tetraethylammonium hydroxide and their subsequent supercritical drying results in a more uniform catalytic material than the one obtained by precipitation with ammonium carbonate and conventional drying. Nevertheless, differences in catalyst preparation and their uniformity had only a small effect on the amounts of all

kinds of cations in the near-surface region of the catalysts and on the course of the reaction of flameless methane combustion.

The modification of manganese–lanthanum oxide catalysts with silver increases the rate of flameless methane combustion. A significant increase in the activity per unit surface area in silver-containing catalysts occurred only for higher reaction temperatures, at which the participation of a new source of oxygen, more weakly bound in the oxides structure in comparison with lattice oxide ions, is possible. Desorption of this kind of oxygen takes place in the temperatures by about 100 K lower than on catalysts without silver. It is probably oxygen released from filled oxygen vacancies in the crystal lattice of oxides, more mobile and easily accessible to methane oxidation. Such defects of the crystal lattice appear due to the great stability of the perovskite structure when substituting lanthanum cations with silver cations. A consequence of filling up oxygen vacancies is the appearance of a larger number of manganese ions in the unstable oxidation state Mn^{4+} in the catalysts. The rate of methane oxidation is a linear function of the Mn^{4+}/Mn^{3+} surface atomic ratio. The value of the Mn^{4+}/Mn^{3+} surface atomic ratio is therefore a significant parameter characterizing the intrinsic properties of the manganese–lanthanum oxides and influencing their activity in the flameless combustion of methane.

The sites of filled oxygen vacancies, providing oxygen for methane combustion, are probably neighboring with silver ions. The remaining part of the catalyst structure, in which oxygen is bound only with manganese ions, may constitute a specific reservoir of oxygen ions with which the vacancies are filled and which is supplemented with the gaseous phase oxygen.

Acknowledgments

The authors acknowledge financial support from the General Secretariat for Research and Technology of Greece and the State Committee for Scientific Research of Poland in the frame of the Polish–Greek Scientific and Technological Programme.

References

[1] H. Arai, A. Machida, Catal. Today 10 (1991) 81.
[2] R.A. Dalla Betta, Catal. Today 35 (1997) 129.
[3] J.G. McCarty, M. Gusman, D.M. Lowe, D.L. Hildenbrand, K.N. Lau, Catal. Today 47 (1999) 5.
[4] L.D. Pfefferle, W.C. Pfefferle, Catal. Rev.-Sci. Eng. 29 (1987) 219, and references cited therein.
[5] D.L. Trimm, Appl. Catal. 7 (1985) 249.
[6] S.R. Vatcha, Energy Convers. Mgmt. 38 (1997) 1327.
[7] A. Machocki, A. Denis, Pol. J. Environ. Stud. 9, Supl. I (2000) 35.
[8] A. Machocki, A. Denis, B. Stasińska, W. Gac, Pol. J. Environ. Stud. 10, Supl. II (2001) 72.
[9] M.F.M. Zwinkels, S.G. Jaras, P.G. Menon, Catal. Rev.-Sci. Eng. 35 (1993) 319, and references cited therein.
[10] T.V. Choudhary, S. Banerjee, V.R. Choudhary, Appl. Catal. A 234 (2002) 1, and references cited therein.
[11] J.G. McCarty, H. Wise, Catal. Today 8 (1990) 231.
[12] L.G. Tejuca, J.L.G. Fierro (Eds.), Properties and Applications of Perovskite-Type Oxides, Dekker, New York, 1993, and references cited therein.
[13] P. Ciambelli, S. Cimino, S. De Rossi, M. Faticanti, L. Lisi, G. Minelli, I. Pettiti, P. Porta, G. Russo, M. Turco, Appl. Catal. B 24 (2000) 243.
[14] H. Arai, T. Yamada, K. Eguchi, T. Seiyama, Appl. Catal. 26 (1986) 265.
[15] T. Seiyama, Catal. Rev.-Sci. Eng. 34 (1992) 281.
[16] R. Spinicci, M. Faticanti, P. Marini, S. De Rossi, P. Porta, J. Mol. Catal. A 197 (2003) 147.
[17] L.A. Isupova, G.M. Alikina, S.V. Tsybulya, A.N. Salanov, N.N. Boldyreva, E.S. Rusina, I.A. Ovsyannikova, V.A. Rogov, R.V. Bunina, V.A. Sadykov, Catal. Today 75 (2002) 305.
[18] L.G. Tejuca, J.L.G. Fierro, J.M.D. Tascon, Adv. Catal. 36 (1989) 237, and references cited therein.
[19] K.S. Song, S.K. Kang, S.D. Kim, Catal. Lett. 49 (1997) 65.
[20] V.R. Choudhary, B.S. Uphade, S.G. Pataskar, G.A. Thite, Chem. Commun. (1996) 1021.
[21] K.S. Song, H.X. Cui, S.D. Kim, S.K. Kang, Catal. Today 47 (1999) 155.
[22] V.R. Choudhary, B.S. Uphade, S.G. Pataskar, Fuel 78 (1999) 919.
[23] S. Ponce, M.A. Pena, J.L.G. Fierro, Appl. Catal. B 24 (2000) 193.
[24] S. Imamura, H. Sawada, K. Uemura, S. Ishida, J. Catal. 109 (1988) 198.
[25] H. Haruta, H. Sano, Stud. Surf. Sci. Catal. 16 (1983) 225.
[26] S.D. Gardner, G.B. Hoflund, D.R. Schryer, J. Schryer, B.T. Upchurch, E.J. Kielin, Langmuir 7 (1991) 2135.
[27] M.-F. Luo, X.-X. Yuan, X.-M. Zheng, Appl. Catal. A 175 (1998) 121.
[28] E. Gulari, C. Guldur, S. Srivannavit, S. Osuwan, Appl. Catal. A 182 (1999) 147.
[29] R. Lin, W.-P. Liu, Y.-J. Zhong, M.-F. Luo, Appl. Catal. A 220 (2001) 165.
[30] X. Wang, Y.-Ch. Xie, React. Kinet. Catal. Lett. 71 (2000) 121.
[31] S. Imamura, S. Yoshie, Y. Ono, J. Catal. 115 (1989) 258.
[32] Lj. Kundakovic, M. Flytzani-Stephanopoulos, Appl. Catal. A 183 (1999) 35.
[33] D. Briggs, M.P. Seah, Practical Surface Analysis by Auger and X-Ray Photoelectron Spectroscopy, Wiley, Chichester, 1983.
[34] B. Klingenberg, M.A. Vannice, Chem. Mater. 8 (1996) 2755.
[35] A. Machocki, T. Ioannides, B. Stasińska, W. Gac, A. Denis, S. Pasieczna, Przem. Chem. 82 (2003) 216.
[36] R.P. Turcotte, J.O. Sawyer, L. Eyring, Inorg. Chem. 8 (1969) 238.
[37] A.J. Nagy, G. Mestl, J. Catal. 188 (1999) 337.
[38] K. Tabata, Y. Hirano, E. Suzuki, Appl. Catal. A 170 (1998) 245.
[39] Y. Ng Lee, R.M. Lago, J.L. Fierro, V. Cortes, F. Sapina, E. Marinez, Appl. Catal. A 207 (2001) 17.
[40] P. Ciambelli, S. Cimino, G. Lasorella, L. Lisi, S. De Rossi, M. Faticanti, G. Minelli, P. Porta, Appl. Catal. B 37 (2002) 231.
[41] M. Daturi, G. Busca, R.J. Willey, Chem. Mater. 7 (1995) 2115.
[42] K. Knizek, M. Daturi, G. Busca, C. Michel, J. Mater. Chem. 8 (1998) 1815.
[43] J.A.M. van Roosmalen, E.H.P. Cordfunke, R.B. Helmoldt, H.W. Zandbergen, J. Solid State Chem. 110 (1994) 100.
[44] S. Castro-Garcia, M. Sanchez-Andujar, C. Rey-Cabezudo, M.A. Senaris-Rodriguez, C. Julien, J. Alloys Compd. 323–324 (2001) 710.
[45] R.A. Nyquist, R.O. Kagel, Infrared Spectra of Inorganic Compounds, vol. 4, Academic Press, San Diego, 1997.
[46] I.S. Smirnova, Phys. B 262 (1999) 247.
[47] O. Carp, L. Patron, A. Ianculescu, J. Pasuk, R. Olar, J. Alloys Compd. 351 (2003) 314.
[48] F. Buciuman, F. Patcas, R. Cracium, D.R.T. Zahn, Phys. Chem. Chem. Phys. 1 (1999) 185.
[49] T.J. Richardson, S.J. Wen, K.A. Striebel, P.N. Ross Jr., E.J. Cairns, Mater. Res. Bull. 32 (1997) 609.

[50] A.A. Davydov, Infrared Spectroscopy of Adsorbed Species on the Surface of Transition Metal Oxides, Wiley, Chichester, 1990.
[51] M. Nieminen, M. Putkonen, L. Niinistö, Appl. Surf. Sci. 174 (2001) 155.
[52] T. Le Van, M. Che, J.M. Tatibouët, M. Kermarec, J. Catal. 142 (1993) 18.
[53] M. O'Connell, A.K. Norman, C.F. Hüttermann, M.A. Morris, Catal. Today 47 (1999) 123.
[54] Y. Zhang-Steenwinkel, J. Beckers, A. Bliek, Appl. Catal. A 235 (2002) 79.
[55] Y. Ng Lee, R.M. Lago, J.L.G. Fierro, J. González, Appl. Catal. A 215 (2001) 245.
[56] Z. Yu, L. Gao, S. Yuan, Y. Wu, J. Chem. Soc., Faraday Trans. 88 (1992) 3245.
[57] G. Sinquin, J.P. Hindermann, C. Petit, A. Kiennemann, Catal. Today 54 (1999) 107.
[58] G. Sinquin, C. Petit, J.P. Hindermann, A. Kiennemann, Catal. Today 70 (2001) 183.
[59] S. Cimino, L. Lisi, R. Pirone, G. Russo, M. Turco, Catal. Today 59 (2000) 19.
[60] S. Cimino, S. Colonna, S. De Rossi, M. Faticanti, L. Lisi, I. Pettiti, P. Porta, J. Catal. 205 (2002) 309.
[61] E.R. Stobbe, B.A. de Boer, J.W. Geus, Catal. Today 47 (1999) 161.
[62] S. Minico, S. Scire, C. Crisafulli, R. Maggiore, S. Galvango, Appl. Catal. B 28 (2000) 245.
[63] S. Scire, S. Minico, C. Crisafulli, S. Galvango, Catal. Commun. 2 (2001) 229.
[64] T. Yamashita, A. Vannice, Appl. Catal. B 13 (1997) 141.
[65] Y. Teraoka, M. Yoshimatsu, N. Yamazoe, T. Seiyama, Chem. Lett. (1985) 893.
[66] A.J. Nagy, G. Mestl, D. Herein, G. Weinberg, E. Kitzelmann, R. Schlögl, J. Catal. 182 (1999) 417.
[67] S. Imamura, Y. Tsuji, Y. Miyake, T. Ito, J. Catal. 151 (1995) 279.
[68] F.C. Buciuman, F. Patcas, T. Hahn, Chem. Eng. Process. 38 (1999) 563.